

## Ferromagnetic fluids

P. C. Hemmer and D. Imbro\*

*Institutt for teoretisk fysikk, Universitetet i Trondheim, N-7034 Trondheim-NTH, Norway*

(Received 14 March 1977)

The equation of state for a system of molecules with exchange interactions in addition to the spin-independent forces is considered, and explicitly evaluated in one and three dimensions for the case of hard-sphere particles with weak long-range forces. Depending upon the ratio  $R$  of the integrated strength of the exchange interaction to the spin-independent attractive interaction, five topologically different phase diagrams occur for the three-dimensional model. The phases involved are magnetic and nonmagnetic solids, magnetic and nonmagnetic liquids, and nonmagnetic gases. Liquid ferromagnetism occurs if the exchange interaction is sufficiently strong,  $R > 0.15$ .

### I. INTRODUCTION

Ferromagnetism, usually associated with matter in the solid state, does also occur in liquids.<sup>1,2</sup> Since magnetic fluids must be described by interacting molecules with both translational and spin degrees of freedom, one is naturally led to consider Hamiltonians of the form

$$H(\{\vec{r}\}, \{\vec{\sigma}\}) = \sum_{i < j} [\varphi(\vec{r}_{ij}) + \vec{\sigma}_i \vec{\sigma}_j \varphi_{\text{ex}}(\vec{r}_{ij})] - \vec{\mathcal{H}} \sum_i \vec{\sigma}_i, \quad (1)$$

where  $\varphi(\vec{r})$  is the spin-independent pair interaction,  $\varphi_{\text{ex}}(\vec{r})$  the exchange integral, and  $\vec{\mathcal{H}}$  an external magnetic field.

For a realistic pair potential  $\varphi(\vec{r})$ , the system would have (at least) two phase transitions, a liquid-gas transition and a liquid-solid transition, in the absence of magnetic interactions ( $\varphi_{\text{ex}} = 0$ ,  $\vec{\mathcal{H}} = 0$ ). The magnetic interaction by itself, assumed ferromagnetic, may, in zero field, induce a phase transition between a nonmagnetic phase and a high-density phase in which the system prefers configurations with a spontaneous magnetization. The present article is a study of the interplay between the spatial ordering encouraged by  $\varphi(\vec{r})$  and the magnetic ordering encouraged by  $\varphi_{\text{ex}}(\vec{r})$ . In particular, we are interested in the topological nature of the phase diagram. How does, for example, the number of phase transitions with the complete Hamiltonian (1) depend upon the relative strengths of the magnetic and the nonmagnetic interactions? Under which conditions do ferromagnetic *liquids* appear (if at all)?

In order to have a tractable model, we assume the molecules to be hard spheres interacting with weak long-range interactions. In Sec. II the model and its equation of state are discussed. The dependence of the phase diagram upon the parameters of the interactions is worked out in detail in Secs. III and IV. We first consider the case in which

both spatial and spin dimensionality is one, since this one-dimensional Ising fluid can be solved exactly. Of course, no fluid-solid transition can occur in this case. In Sec. IV the case in which spatial and spin dimensionality is three is considered, with an isotropic classical Heisenberg exchange interaction. The resulting equation of state contains as one ingredient the hard-sphere equation of state, for which we use the well-known molecular dynamics and Monte Carlo results. The phase diagram for the three-dimensional model has a richer structure than the one-dimensional version due to the existence of the hard-sphere transition.

In both cases, the topology of the phase diagram depends upon one physical parameter: the ratio  $R$  of the integrated strengths of the nonmagnetic and magnetic long-range interactions,

$$R = \frac{\int \varphi_{\text{ex}}(\vec{r}) d\vec{r}}{\int \varphi_{\text{attr}}(\vec{r}) d\vec{r}}. \quad (2)$$

In the three-dimensional case there are, in zero field, five topologically different phase diagrams (exhibited in Fig. 6), each corresponding to a range of  $R$  values. For  $0 < R < R_4$ , the ferromagnetic transition takes place entirely within the solid phase. For  $R_4 < R < R_3$  (and in a definite range of pressures), the solid stays ferromagnetic all the way up to the melting temperature; in other words, a transition between a ferromagnetic solid and a nonmagnetic liquid takes place. For  $R > R_3$ , a ferromagnetic liquid appears. In a range  $R_3 < R < R_2$  the transition between a ferromagnetic and a nonmagnetic fluid occurs with a discontinuity in the compressibility, while for  $R_2 < R < R_1$  this transition goes, at a tricritical point  $M$ , over into a first-order magnetic transition at lower temperatures. In this range the maximum number of phases appear in the phase diagram: nonmagnetic gas, nonmagnetic and magnetic liquids, and nonmagnetic and magnetic solids. Finally, when  $R > R_1$  the exchange interaction is completely domi-

nant so that the transition between nonmagnetic liquid and nonmagnetic gas, including the ordinary gas-liquid critical point  $C$ , has disappeared. Numerical values for the borderline interaction ratios  $R_1$ ,  $R_2$ ,  $R_3$ , and  $R_4$  are given.

Since the configurational disorder is brought about by thermal motions and characterized by an equilibrium temperature  $T$ , magnetic fluids must of course be classified as completely *annealed* (rather than quenched) disordered magnetic systems.

## II. MODEL

We consider a  $d$ -dimensional spin fluid with the interaction energy (1). The spin-independent pair interaction  $\varphi(\vec{r})$  represents a hard core of diameter  $d$  plus a weak attraction of long range:

$$\varphi(\mathbf{r}) = \begin{cases} \infty, & r < d \\ \varphi_{\text{attr}}(\vec{r}) = -\gamma^d a(\gamma\vec{r}), & \text{otherwise,} \end{cases} \quad (3)$$

where the integral of the attractive potential,

$$a \equiv \gamma^d \int a(\gamma\vec{r}) d\vec{r}, \quad (4)$$

is assumed to exist and be positive. Positivity is required if the fluid is to possess a gas-liquid transition, since the essential mechanism of condensation is the competition between liquid configurations of low energy and gaseous configurations with large entropy.

The magnetic interaction is also assumed to be weak and long-ranged,

$$\varphi_{\text{ex}}(\vec{r}) = -\gamma^d a_m(\gamma\vec{r}), \quad (5)$$

again with the requirement that

$$a_m \equiv \gamma^d \int a_m(\gamma\vec{r}) d\vec{r} \quad (6)$$

exists and is positive. Here positivity implies that the spins interact ferromagnetically.

Only the limit in which the inverse range  $\gamma$  approaches zero (after the thermodynamic limit is taken) is considered here. The treatment of these weak long-range forces is well known.<sup>3</sup> The nonmagnetic case  $\varphi_{\text{ex}}(\vec{r}) = 0$  leads, as demonstrated by van Kampen<sup>4</sup> and proved by Lebowitz and Penrose,<sup>5</sup> to a van der Waals-like equation of state. On the other hand, the purely magnetic interaction leads, for localized spins, to a Weiss magnetic equation of state.<sup>6</sup>

These results are rigorous<sup>5,7</sup> in the limit  $\gamma \rightarrow 0$ , and are also easily derived heuristically by recognizing that the weakness and the long range of the  $\gamma$ -parametrized potentials imply that these interactions have essentially no influence on the particle correlations, while still contributing to

the energy.

For our case we only present a similar heuristic derivation, since a rigorous proof, generalizing well-known derivations,<sup>5,7,8</sup> will, under some restrictions on  $a(\vec{r})$  and  $a_m(\vec{r})$ , doubtlessly yield the same result.

Consider first a system of  $N$  particles with a fixed total magnetization  $Nm$  in a volume  $N\rho$ . The energy contribution from the long-ranged potentials in (1) amounts to

$$-\frac{1}{2} N \rho m^2 a_m - \frac{1}{2} N \rho a \quad (7)$$

for almost all configurations [ $N \gg \gamma^{-1}$  is assumed and Eqs. (4) and (6) are used].

Adding the field energy

$$-N \vec{\mathcal{C}} \cdot \vec{m}, \quad (8)$$

we can relate the free energy per particle,  $f(\rho, \vec{m}, T, \vec{\mathcal{C}})$ , to the free energy with no long-range interactions and zero field,  $f_0(\rho, m, T)$ :

$$f(\rho, \vec{m}, T, \vec{\mathcal{C}}) = f_0(\rho, \vec{m}, T) - \frac{1}{2} \rho m^2 a_m - \frac{1}{2} \rho a - \vec{\mathcal{C}} \cdot \vec{m}. \quad (9)$$

For the system with *unrestricted* magnetization, the actual free energy  $f(\rho, T, \vec{\mathcal{C}})$  is the minimum of (9) with respect to  $\vec{m}$ :

$$f(\rho, T, \vec{\mathcal{C}}) = \inf_{|\vec{m}| \leq 1} [f_0(\rho, m, T) - \frac{1}{2} \rho m^2 a_m - \frac{1}{2} \rho a - \vec{\mathcal{C}} \cdot \vec{m}]. \quad (10)$$

Since  $f_0(\rho, m, T)$  represents a reference system in which the spatial and spin degrees of freedom are decoupled, this free energy is composed of two additive contributions, a hard-sphere free energy  $f_h(\rho, T)$  and a free-spin part  $f_s(m, T)$ , the latter a pure entropy contribution:

$$f(\rho, T, \vec{\mathcal{C}}) = \inf_{|\vec{m}| \leq 1} [f_s(\vec{m}, T) + f_h(\rho, T) - \frac{1}{2} a_m m^2 \rho - \frac{1}{2} a \rho - \vec{\mathcal{C}} \cdot \vec{m}]. \quad (11)$$

The extremum in (11) is obtained for a magnetization  $\vec{m}$  (parallel to  $\vec{\mathcal{C}}$ ) that satisfies

$$\frac{\partial f_s}{\partial m} = \vec{\mathcal{C}} + a_m \rho m. \quad (12)$$

This may be expressed as an effective-field equation of state,

$$m = m_s(\vec{\mathcal{C}} + a_m \rho m, T), \quad (13)$$

where the function  $m_s(\vec{\mathcal{C}}, T)$  describes the magnetization curves for free spins.

The pressure follows from (11) as

$$p(\rho, T) = \rho^2 (\partial f / \partial \rho)_T = \text{MC} [p_h(\rho, T) - \frac{1}{2} a_m \rho^2 m^2 - \frac{1}{2} a \rho^2], \quad (14)$$

where  $m$  now corresponds to the extremum. By (12) there is no contribution from the implicit density dependence through  $m(\rho)$ . The right-hand side of Eq. (14) has been supplemented with the Maxwell equal-area construction (MC) in order that the free energy should be a convex function of the volume. (In the rigorous derivations the Maxwell rule comes automatically.)

For the special case of  $a=0$  and Ising spins, a rigorous proof of these results was supplied by Frankel and Thompson.<sup>8</sup>

The coupled equations (13) and (14), supplied with the appropriate free-spin magnetization  $m_s(\mathcal{H}, T)$  and the hard-core equation of state in the relevant dimension,  $p_h(\rho, T)$ , form the basis for the subsequent discussions.

### III. ONE-DIMENSIONAL CASE

A system of hard-core particles in one dimension obeys Tonks' equation of state,

$$p_h(\rho, T) = kT\rho(1 - \rho d)^{-1}, \quad (15)$$

while noninteracting spins with one degree of freedom (Ising spins) have a magnetic moment per spin equal to

$$m_s(\mathcal{H}, T) = \tanh(\mathcal{H}/kT). \quad (16)$$

Hence the thermodynamic equation of state (14) takes the explicit form

$$p(\rho, T) = \text{MC}[\hat{p}(\rho, T)], \quad (17)$$

$$\hat{p}(\rho, T) = kT\rho(1 - \rho d)^{-1} - \frac{1}{2}a_m\rho^2m^2 - \frac{1}{2}a\rho^2, \quad (18)$$

in this case. Here  $m = m(\rho, T)$  satisfies the Weiss equation

$$m = \tanh[(\mathcal{H} + a_m\rho m)/kT]. \quad (19)$$

Let us now study the thermodynamics of this fluid for  $\mathcal{H}=0$ . In zero field, *two* regions exist, one in which the fluid is nonmagnetic, and a colder and denser region in which a nonzero spontaneous magnetization appears:

$$m = \begin{cases} 0 & \text{for } a_m\rho < kT \\ m_0(\rho, T) & \text{for } a_m\rho > kT. \end{cases} \quad (20)$$

Across the transition line  $kT = a_m\rho$ , the function  $\hat{p}(\rho, T)$  is continuous, whereas the isothermal compressibility is discontinuous. The discontinuity in slope of an isotherm equals

$$\left(\frac{\partial \hat{p}}{\partial \rho}\right)_{\text{NONMAG}} - \left(\frac{\partial \hat{p}}{\partial \rho}\right)_{\text{MAG}} = \frac{a_m\rho^2}{2} \left(\frac{\partial m_0^2}{\partial \rho}\right)_T = \frac{3}{2}kT, \quad (21)$$

since in zero field, Eq. (19) behaves asymptotically as

$$m_0^2(\rho, T) \approx 3a_m\rho/kT - 3 \quad (22)$$

near the Curie point.

The nature of this magnetic transition in the absence of attractive forces ( $a=0$ ) is easily discussed, and is summarized in Fig. 1: At temperatures  $T > a_mk^{-1}d^{-1}$  no such transition exists; at lower temperatures a transition with discontinuous compressibility (cusped isotherms) occurs. Since the numerical coefficient on the right-hand side of (21) exceeds unity, the derivative on the high-density (magnetic) side of the transition,

$$\left(\frac{\partial \hat{p}}{\partial \rho}\right)_T = kT(1 - \rho d)^{-2} - \frac{3}{2}kT, \quad (23)$$

becomes negative at sufficiently low temperatures, in which case a *first-order* transition takes place. The changeover occurs at a magnetic tricritical point  $M$ ,

$$\rho_M d = kT_M d/a_m = (3 + \sqrt{6})^{-1}, \quad (24)$$

$$p_M = a_m d^{-2}(12 + 5\sqrt{6})^{-1}.$$

$M$  is called "tricritical" since (with an added field

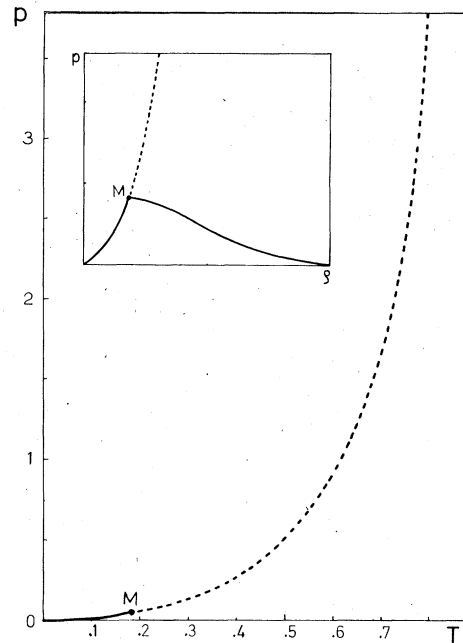


FIG. 1. Phase diagram for the one-dimensional model in zero field and with no attraction ( $a=0$ ). Temperatures are measured in units of  $a_mk^{-1}d^{-1}$ , pressures in units of  $a_md^{-2}$ . For all  $T < 1$  a transition between a magnetic and a nonmagnetic phase takes place. For  $T < T_M$  this is a first-order transition. For  $T > T_M$  the location of the transition is given by  $p = T^2(1 - T)^{-1}$  in our units. The pressure-density diagram is shown in the insert. The coexistence curve for the first-order transition is drawn with solid lines.

axis) three phases become identical at this point: the nonmagnetic phase and the spin-up and spin-down magnetic phases. A more detailed discussion of this special case is contained in Ref. 8.

The other special case of no magnetic interaction yields van der Waals's equation of state with a gas-liquid critical point  $C$  at

$$\rho_C = \frac{1}{3}d^{-1}, \quad kT_C = \frac{4}{27}ad^{-1}, \quad p_C = \frac{1}{54}ad^{-2}. \quad (25)$$

Turning now to the complete equation of state (17), we note that it depends nontrivially upon just *one* parameter: the ratio between the strengths of the magnetic and the nonmagnetic interactions,

$$R = a_m/a. \quad (26)$$

This is immediately apparent when one expresses densities, temperatures, and pressures in units of  $d^{-1}$ ,  $ak^{-1}d^{-1}$ , and  $ad^{-2}$ , respectively. For given values of  $R$ , one easily calculates the function  $\hat{p}(\rho, T)$ , Eq. (18), numerically and, by a Maxwell construction, the pressure  $p$ . In Fig. 2 characteristic isotherms for  $\hat{p}$  and  $p$  as functions of the volume  $v = \rho^{-1}$  are shown for the special value  $R = 0.26$ . This value of  $R$  is chosen to exemplify an interaction for which both critical points  $M$  and  $C$  appear. Figure 3 shows the corresponding  $p$ - $T$  diagram together with the coexisting densities.

Since the gas-liquid critical point  $C$  occurs in the *nonmagnetic* region, these critical parameters are still given by Eq. (25). The magnetic tricritical point  $M$  is here located at almost the same temperature,  $T_M \approx 0.996T_C$ , but at considerably higher density and pressure,  $\rho_M \approx 1.70\rho_C$  and  $p_M \approx 1.76p_C$ . For other values of  $R$  the tricritical density  $\rho_M$  and temperature  $T_M$  are given by

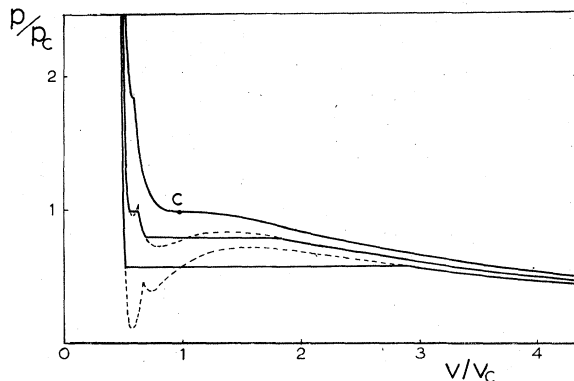


FIG. 2. Zero-field isotherms for the one-dimensional model with an interaction ratio  $R = 0.26$ . The dashed line shows  $\hat{p}(\rho, T)$  when this function does not coincide with the pressure. The magnetic critical point is located at  $T_M = 0.996 T_C$ ,  $p_M = 1.70 p_C$ , and  $V_M = 0.59 V_C$ . The three isotherms corresponds to temperatures  $T_C$ ,  $0.95 T_C$ , and  $0.90 T_C$ , and exhibit zero, two, and one first-order transitions, respectively.

$$\rho_M d = 1 - \left(\frac{3}{2} + R^{-1}\right)^{-1/2},$$

$$kT_M d/a = R - R\left(\frac{3}{2} + R^{-1}\right)^{-1/2}. \quad (27)$$

From Fig. 3 we see, moreover, that the magnetic and nonmagnetic first-order transitions merge at a lower pressure:  $p_B \approx 0.76p_C$ . At this triple point  $B$  nonmagnetic gas, nonmagnetic liquid, and magnetic liquid coexist, while at lower temperatures the nonmagnetic gas condenses directly to a magnetic liquid upon compression.

The magnetic transition line at high temperatures ( $T > T_M$ ) is easily shown to be given by

$$\frac{p}{p_C} = \left(\frac{T}{T_C}\right)^2 \left(\frac{32}{27R - 4T/T_C} - \frac{16}{27}R^{-2}\right) \quad (28)$$

by combining Eqs. (18), (20), (25), and (26).

If now  $R$  is lowered, i.e., the magnetic interaction is weakened, the magnetic first-order transition takes place at lower and lower temperatures according to Eq. (27), while the gas-liquid vapor pressure curve for  $T_B < T < T_C$  is unaffected.

Therefore the magnetic tricritical point  $M$  must finally hit the evaporation curve for the liquid-gas transition. One decides easily when this happens by investigating whether the cusp on the isotherm  $T = T_M$  lies within the Maxwell construction connected with the van der Waals transition. This is found to be the case for  $R < R_2 \approx 0.211$ . For  $R < R_2$  the tricritical point  $M$  has disappeared. The non-

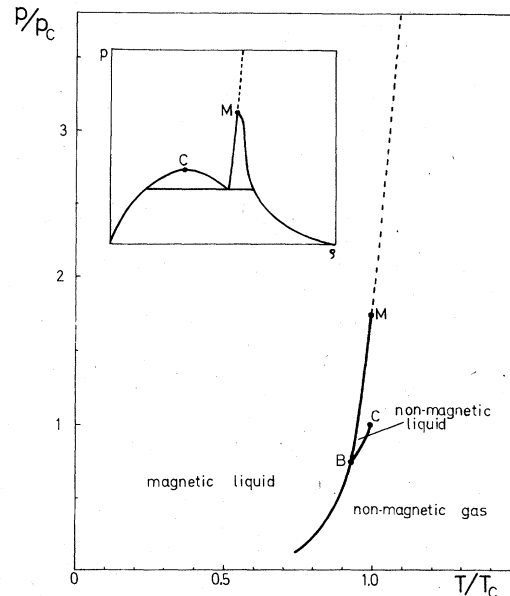


FIG. 3. Zero-field phase diagram for the one-dimensional model with an interaction ratio  $R = 0.26$ . First-order transitions are shown as solid lines. The pressure-density diagram is shown in the insert. The coexistence curve for the first-order transition is drawn with solid lines.

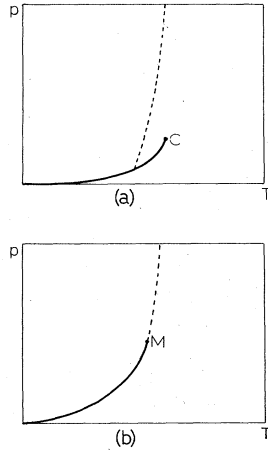


FIG. 4. Typical phase diagrams for the one-dimensional model (in zero field) for (a)  $R < R_2 \approx 0.211$  and (b)  $R > R_1 \approx 0.304$ . First-order transitions are shown as solid lines.

magnetic gas may still condense into a magnetic or a nonmagnetic liquid, depending upon the temperature [see Fig. 4(a)].

If, on the other hand, one starts with a situation with both critical points  $C$  and  $M$  present (Fig. 3, for instance) and *strengthens* the magnetic interaction by increasing  $R$ , the coexistence curve connected with the magnetic first-order transition becomes wider and the nonmagnetic gas-liquid transition is eventually engulfed in this magnetic transition. One detects easily the value  $R_1$  for which this happens by studying the isotherm  $T = T_C = 4a/27kd$  for increasing  $R$  and noting when the critical point  $C$  disappears into the Maxwell construction connected with the magnetic transition. We find this to occur for  $R = R_1 \approx 0.304$ . For  $R > R_1$  the liquid is always magnetic [Fig. 4(b)].

Thus the one-dimensional fluid possesses two first-order phase transitions only when the types of interactions balance each other so that the interaction ratio is kept within the narrow range

$$R \in (R_2, R_1) \approx (0.211, 0.304). \quad (29)$$

#### IV. THREE DIMENSIONS

We now consider a three-dimensional fluid with an isotropic classical Heisenberg interaction. The magnetization of *free* classical vector spins is then described by the well-known Langevin function

$$m_s(\mathcal{H}, T) = L(\mathcal{H}/kT), \quad (30)$$

with

$$L(x) = \coth x - x^{-1}. \quad (31)$$

The magnetic part of the equation of state, Eq. (13), therefore takes the explicit form

$$m = L(a_m \rho m / kT) \quad (32)$$

in zero field. The criterion for the presence of a

spontaneous magnetization,  $a_m \rho > 3kT$ , is qualitatively the same as in the one-dimensional case.

The equation of state for hard spheres,  $p_h(\rho, T)$ , is not known exactly, but careful Monte Carlo and molecular-dynamics evaluations<sup>9</sup> of it exist.

These computer studies show that the hard-sphere system exhibits a fluid-solid transition. We use the Carnahan-Starling<sup>10</sup> analytic representation of the fluid branch,

$$p_h(\rho, T) = kT\rho(1 + \eta + \eta^2 - \eta^3)(1 - \eta)^{-3}, \quad (33)$$

where

$$\eta = \frac{1}{6} \pi \rho d^3. \quad (34)$$

This representation, which is an interpolation between the Percus-Yevick compressibility and virial-equation results, fits the numerical results extraordinarily well and reproduces all the known virial coefficients with great precision. For the solid branch we use the Hall parametrization [Eq. (12) of Ref. 11] with a tie line at  $p/kT = 11.6d^{-3}$ .

In this case, one expects the system to have two or three first-order transitions, and this is indeed so. As for the one-dimensional model the gas-liquid transition and the magnetic first-order transition can only appear simultaneously if the two types of interaction are not too disproportionate. By the same procedure as in the one-dimensional case, one finds that the interaction ratio must be restricted to the interval

$$R \in (R_2, R_1) \approx (0.38, 0.63) \quad (35)$$

to have both these first-order transitions, i.e., a total of three first-order transitions, appearing.

In Fig. 5 we show the full phase diagram for an interaction ratio  $R$  in this range,  $R = 0.50$ . A total of five different phases appear: nonmagnetic gas, liquid, and solid phases, together with magnetic liquid and solid phases. We note the presence of both critical points  $C$  and  $M$ , as expected, together with two triple points  $A$  and  $B$  and two points  $D$  and  $E$  on the melting line for which a solid and a liquid phase coexist, but in addition they are points at which the magnetic and nonmagnetic varieties of one of the condensed phases become identical (liquid phases for  $D$ , solid phases for  $E$ ). When the temperature lies between  $T_D$  and  $T_E$ , the density corresponding to the magnetic transition,

$$\rho = 3kT/aR, \quad (36)$$

lies within the Maxwell construction connected with the melting transition.

For varying interaction ratios  $R$ , five topologically different phase diagrams are encountered for our three-dimensional model. They are sketched in Fig. 6.

For  $R > R_1 \approx 0.63$  only the magnetic transition and

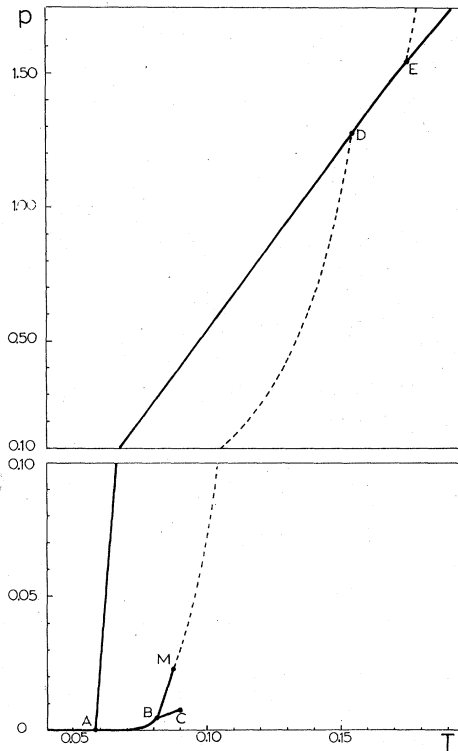


FIG. 5. The zero-field phase diagram for the three-dimensional model with an interaction ratio  $R = 0.50$ . The nature of the phases is explained in the text and in Fig. 6(b). Pressures are measured in units of  $ad^{-3}$ , temperatures in units of  $ak^{-1}d^{-6}$ .

the hard-sphere transition are present, corresponding to two fluid and two solid phases, one of each kind being magnetic, the other nonmagnetic. For  $R \in (R_3, R_2) \approx (0.15, 0.38)$  the magnetic first-order transition (and therefore the tricritical point  $M$ ) has disappeared, but all five phases are still present. For  $R \in (R_4, R_3) \approx (0.12, 0.15)$  the magnetic liquid phase has disappeared, while the solid at melting is either ferromagnetic (for temperatures  $T_A < T < T_E$ ) or nonmagnetic (for temperatures above  $T_E$ ). Finally, for  $R \in (0, R_4) \approx (0, 0.12)$  the solid is always nonmagnetic at melting; the magnetic transition takes place entirely within the solid phase. Now the triple point  $A$ , at

$$T_A \approx 0.042ak^{-1}d^{-6}, \quad \rho_A = 1.086d^{-3}, \quad (37)$$

is unaffected by the exchange interaction, and in the nonmagnetic region this is essentially the model proposed by Longuet-Higgins and Widom<sup>13</sup> to describe the triple point of argon.

## V. CONCLUDING COMMENTS

We have seen in Sec. IV that in three dimensions the Hamiltonian (1) allows, for a certain range of

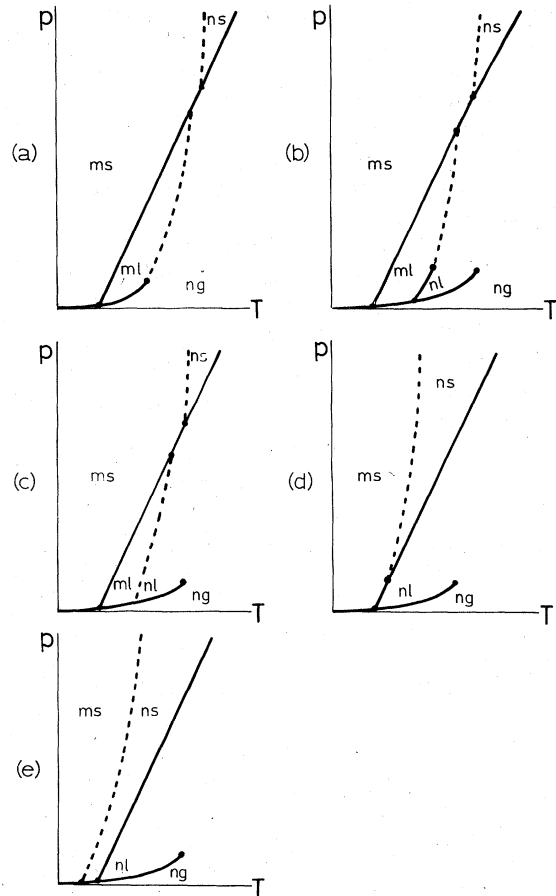


FIG. 6. The five different types of phase diagrams for the three-dimensional model (in zero field). The different phases are denoted as follows: ng, nonmagnetic gas; nl, nonmagnetic liquid; ml, magnetic liquid; ns, nonmagnetic solid; and ms, magnetic solid. The diagrams correspond to the following ranges of the interaction ratio  $R$ : (a)  $R > R_1$ , (b)  $R_2 < R < R_1$ , (c)  $R_3 < R < R_2$ , (d)  $R_4 < R < R_3$ , and (e)  $0 < R < R_4$ . (The numerical values are  $R_1 \approx 0.63$ ,  $R_2 \approx 0.38$ ,  $R_3 \approx 0.15$ , and  $R_4 \approx 0.12$ ).

interaction parameters, as much as five different phases, two of these being condensed magnetic phases. A ferromagnetic *liquid* phase is present only if the total integrated strength of the exchange interaction is not too small compared with the strength of the nonmagnetic attraction (at least 15% of it).

We note that a molecular-field treatment of a model with *short-range* forces would yield identical results with our exact calculation for weak long-range forces. We believe that the present mean-field criterion for fluid magnetism,

$$\frac{\int \varphi_{\text{ex}}(\vec{r}) d\vec{r}}{\int \varphi_{\text{atr}}(\vec{r}) d\vec{r}} > 0.15, \quad (38)$$

is still valid for a more realistic interaction in a

qualitative and perhaps even semiquantitative sense.

Liquid ferromagnetism is so far only observed<sup>1,2</sup> in liquid *mixtures* (AuCo alloys). Since mixtures with weak long-range forces can be treated<sup>1,2</sup> exactly to dominant orders, there is in principle no difficulty in generalizing the present treatment to that case.

Finally we note that we have only treated the case when the external magnetic field vanishes. This is the most interesting case because the ferromagnetic transition occurs for  $\mathcal{H} = 0$ . One can envisage what happens in nonzero fields by first considering very strong fields. Then the magnetization  $m$  is almost unity (except at ex-

tremely high temperatures), and the magnetic contribution to the pressure,  $-\frac{1}{2}a_m\rho^2m^2$ , can be considered as a mere addition to the nonmagnetic contribution,  $-\frac{1}{2}a\rho^2$ . This means that at strong fields one sees (except at very high temperatures) a constant saturated magnetization together with the nonmagnetic equation of state, where temperatures and pressures are scaled by a factor of  $1 + a_m/a$ . In a phase diagram of the type shown in Fig. 6, the gas-liquid and magnetic first-order transitions will both be present for small fields, but will merge when the field is increased or decreased from zero. The magnetic transition with a discontinuous isothermal compressibility will, on the other hand, be present *only* in zero field.

---

\*Present address: Lawrence Livermore Laboratory, University of California, P. O. Box 808, Livermore, Calif. 94550.

<sup>1</sup>G. Busch and H. J. Guentherodt, *Phys. Lett.* **A27**, 110 (1968).

<sup>2</sup>B. Kraeft and H. Alexander, *Phys. Kondens. Mater.* **16**, 281 (1973).

<sup>3</sup>For a review, see P. C. Hemmer and J. L. Lebowitz, in *Phase Transitions and Critical Phenomena*, edited by C. Domb and M. S. Green (Academic, London, 1976), Vol. 5B, Chap. 2, p. 107.

<sup>4</sup>N. G. van Kampen, *Phys. Rev.* **135**, A362 (1964).

<sup>5</sup>J. L. Lebowitz and O. Penrose, *J. Math. Phys.* **7**, 98 (1966).

<sup>6</sup>R. Brout, *Phase Transitions* (Benjamin, New York,

1965).

<sup>7</sup>D. J. Gates and O. Penrose, *Commun. Math. Phys.* **15**, 255 (1969).

<sup>8</sup>N. E. Frankel and C. J. Thompson, *J. Phys. C* **8**, 3194 (1975).

<sup>9</sup>W. W. Wood and T. D. Jacobson, *J. Chem. Phys.* **27**, 1207 (1957); B. J. Alder and T. E. Wainwright, *J. Chem. Phys.* **27**, 1208 (1957).

<sup>10</sup>N. F. Carnahan and K. E. Starling, *J. Chem. Phys.* **51**, 635 (1969).

<sup>11</sup>K. Hall, *J. Chem. Phys.* **57**, 2252 (1972).

<sup>12</sup>E. H. Hauge, *J. Chem. Phys.* **44**, 2249 (1966).

<sup>13</sup>H. C. Longuet-Higgins and B. Widom, *Mol. Phys.* **8**, 549 (1965).